

Article

Design, Analysis and Simulation of Microstrip Antenna Arrays with Flexible Substrate in Different Frequency, for Use in UAV-Assisted Marine Communications

Leopoldo Gómez ^{1,*} and Ahmed S. Ibrahim ²

¹ Escuela Superior de Ingeniería, Universidad de Cádiz, 11519 Puerto Real, Spain

² Electrical and Computer Engineering Department, Florida International University, Miami, FL 33199, USA

* Correspondence: leopoldo.gomez@uca.es; Tel.: +34-659-64-88-23

Abstract: The maritime land–sea communication channel experiences multipath shadowing and fading due to ships, onshore and offshore structures, and reflections from the sea surface. When using low altitude antennas, the sea surface itself can block the propagation of radio waves when the first Fresnel zone is obstructed. The latter can occur within a few kilometres of the transmitter at microwave frequencies. Sea reflections are stronger than ground reflections due to the higher conductivity of the sea, leading to more interference problems. In this paper, a microwave frequency patch antenna array is analysed, designed, and simulated for a novel system to improve marine communications to be applied by unmanned aerial vehicles (UAVs). The patch antenna array with flexible substrate will be studied with different frequencies. In this way, the test will check and obtain the best characteristics for an antenna that is built into the UAV with CTS studio.

Keywords: patch antenna array; UAV; flexible substrate; marine communications



Citation: Gómez, L.; Ibrahim, A.S. Design, Analysis and Simulation of Microstrip Antenna Arrays with Flexible Substrate in Different Frequency, for Use in UAV-Assisted Marine Communications. *J. Mar. Sci. Eng.* **2023**, *11*, 730. <https://doi.org/10.3390/jmse11040730>

Academic Editors: Kazem Reza Kashyzadeh and Okan Unal

Received: 14 February 2023

Revised: 22 March 2023

Accepted: 25 March 2023

Published: 27 March 2023



Copyright: © 2023 by the authors. Licensee MDPI, Basel, Switzerland. This article is an open access article distributed under the terms and conditions of the Creative Commons Attribution (CC BY) license (<https://creativecommons.org/licenses/by/4.0/>).

1. Introduction

Monitoring the marine environment is very important for maintaining such delicate ecosystems, which directly affects local climates, flora, fauna, and human activities. Such monitoring plays a key role in their preservation, which is most commonly done using environmental sensing buoy networks.

Marine communications between land base stations and boats, as shown in Figure 1, are generally needed to provide voice and data exchange services. However, there are often quite a few problems in maritime communications, such as the shadows of the various obstacles located among the points to be communicated, and the reflections from the sea surface [1]. Experimental measurements made so far highlight that one of the problems of marine communication is the low height of on-board antennas [2–4], and another is the low efficiency of these antennas. If the height of the antenna is not high enough above sea level and the antenna design is not optimum, there will be a considerable power loss, which will weaken the signal to the point that there will be no communication among the nodes of the communications network [5].

UAVs [6] can be used to enhance marine communications. For instance, it can be seen as an extremely low orbit satellite relaying the signal between the boat and the base station or other boats. This is intended to combat the fading phenomena described above. A UAV [7] relay can also send data from a source sensor to a remote base station (BS) to minimize the average outage probability along the three-dimensional (3D) UAV. Additionally, UAVs are used as systems of analysis, as nodes in free-space optical (FSO), with the amplify-and-forward relaying protocol and intensity modulation/direct detection technique [8], and investigation in an asymmetric, dual-hop radio frequency (RF)/FSO system with the amplified-and-forward relay protocol for the Space-air-ground integrated networks (SAGIN) [9].

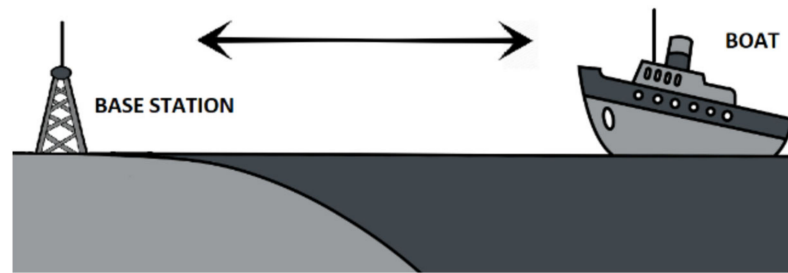


Figure 1. First communication scenario representing the communication between a boat and a base station.

In this paper, we will prove that increasing the height of maritime communication antennas, by deploying a UAV at high altitude, considerably decreases the impact of multipath and shadowing fading [10]. This is because when the height of the antennas is increased, the free space of the first Fresnel zone is larger. Consequently, possible obstacles between the transmitting and receiving antenna can be overcome, which results in a minimisation of the shadow fading effect. In addition, reflections from the sea surface will be less severe because the angle of incidence of the radio wave will be larger.

Together with the UAVs, installing an antenna with optimal properties on the UAV airframe will be equivalent to installing it at a higher altitude (100 m or more). The design of the antenna is an important point for improving maritime communications, being capable of maximising its efficiency can achieve a long transmission distance without losses. Therefore, in the second part of the work, several antennas with different models and frequencies will be studied, designed, and analysed. The results will then be compared, and the work will conclude with the fabrication of the most optimal antenna. However, it is very difficult to design an antenna that radiates 360 degrees in all directions of a UAV, because the substrate is flat and rigid, and the antenna does not radiate equally on both sides as well. For this reason, we are going to study, analyse, and simulate a microstrip array antenna with flexible substrate [11–17], which can be installed on the UAV, and adding a new aspect to the design. The different types of flexible substrates available will be studied to check which of them have the best characteristics for the antenna, since these substrates are not commonly used nowadays.

Finally, simulations of a set of 2×1 antenna patch arrays [18–30] will be performed with the program CST Studio [31], step by step, with the previously chosen flexible substrate and with different frequencies, to check their advantages and disadvantages in each sector, finally performing an adjustment of the antenna array in order to make a design with the maximum performance for each frequency sector.

In summary, the main objective of this paper is the design, simulation, and analysis of a microstrip array antenna with different microstrip matching networks and different frequencies in CST Studio, to achieve a reliable and optimal antenna for its use in maritime communications assisted by UAVs, confirming with a study in MATLAB, that thanks to the UAVs, the significant bit error of the signal decreases in rate.

The rest of this paper is organized as follows.

- In Section 2, we describe the effectiveness of using an UAV to improve marine communications.
- In Section 3, a design of a patch antenna is made according to the equations obtained in the bibliography, and finally, with the support of simulations with CST Studio, an analysis is made to improve its characteristics. The analysis is made for one frequency antennas of two different frequencies and feeds, in order to compare and choose the one with the best final characteristics.
- In Section 4, a similar analysis is performed as in Section 3, but for a 2×1 patch antenna array.
- Section 5 explains the conclusions of the paper and suggests directions for future work.
- Finally, references are given at the end of the paper.

2. UAV Based Model

The UAV is a device that is used today for many applications. One of them is to improve communications through use as communication nodes, between a transmitter and a base station, for instance.

In our paper, the UAV is used for a marine communications application, serving as a node between a base station and a ship, and a patch antenna array with optimal properties for lossless transmission is installed in its casing.

Firstly, three different marine communication scenarios will be compared by simulating the transmission loss of each one. The scenarios are described as follows.

The first scenario is shown in Figure 1 and represents the radio link between a boat and a base station. This is the basic scenario for the simulation. A height of 4 m is considered for both on-board and onshore antennas, which are 1 Km apart from each other. We will suppose, for simplicity, that there is not any special source of shadowing affecting communication, except the sea surface. Thus, only the multipath effect will be taken into account.

In the second scenario, a signal repeater is located in the middle point between the boat and the base station, so that the radio link is divided, just as the radio link described in the first scenario, into two radio links of 500 m length each one. The repeater is installed aboard a buoy. All the system nodes have 4-m-high antennas. This scenario is shown in Figure 2.

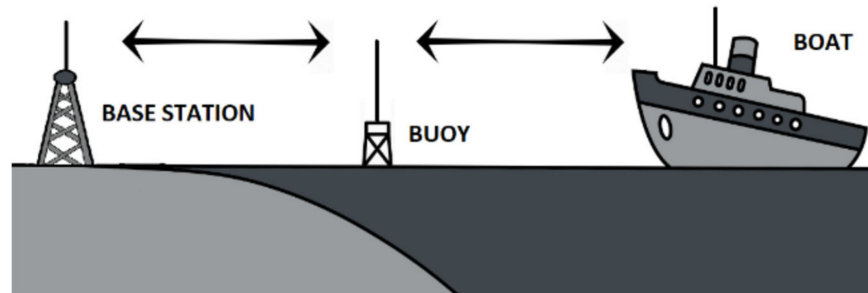


Figure 2. Second communication scenario in which a buoy performs the role of intermediary between the boat and the base station.

The third communication scenario is the novel scenario proposed in this paper. It will be carried out using an UAV as an elevated platform to the repeater. In the simulation, we will set the height of the UAV, and therefore of the repeater antenna, at 185 m. The UAV remains flying over a fix point located on the deck of the boat. We again set a radio link with two sections, but here, one of them is the base station to UAV section and the other one is the UAV to boat section. We will keep the 4-m-high antennas to base station and boat, as in the scenarios before. The same distance between the base station and the boat (1 Km) is also considered. Figure 3 shows the novel scenario.

2.1. Large-Scale Fading Numerical Results

In this subsection, the received mean power at the base station is calculated for each of the three communication scenarios described previously, as follows [3,4]:

$$P_{RX}(d) = P_{RX}(d_0) - 10\gamma \log_{10}(d/d_0) - X_{\sigma}, \tag{1}$$

In Equation (1), $P_{RX}(d_0)$ denotes the expected level of received mean power at the reference distance d_0 (10 m in our calculation), γ denotes the loss exponent of the path, and X_{σ} represents the shadow fading effect that is generally modelled as a zero-mean Gaussian (normal) distributed random variable (in dB) with standard deviation σ dB, as can be seen in the following equation:

$$X_{\sigma} \sim N(0, \sigma), \tag{2}$$

In the calculations, $\gamma = 3.4$ and $\sigma = 5.5$ dB for both the base station to boat and base station to buoy links are taken, and $\gamma = 2.7$ and $\sigma = 4.9$ dB for the buoy to boat link [6]. For UAV to base station link, $\gamma = 2.1$ and $\sigma = 3.4$ dB is used [5], and for UAV to boat link, free space conditions were considered. The frequency was taken at 5.8 GHz. The results of different scenarios can be compared in the Table 1.

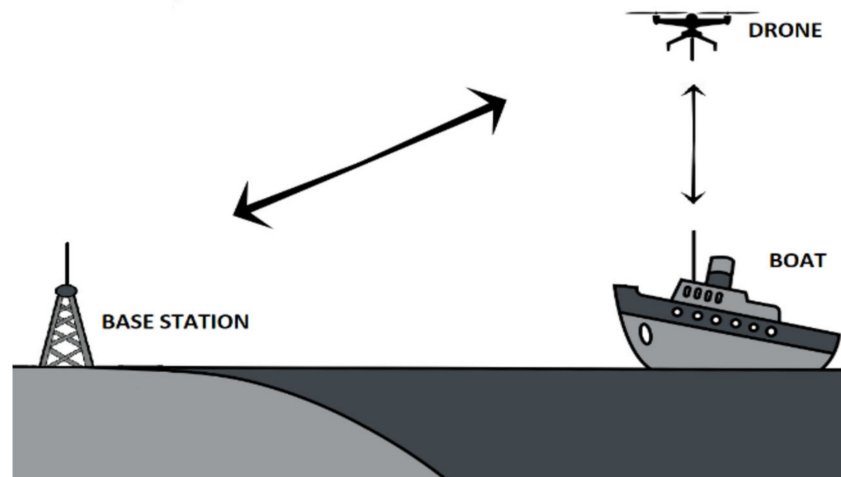


Figure 3. Third communication scenario including an UAV, which performs the role of intermediary between the boat and the base station.

Table 1. Summarizes the results to the different scenarios.

Scenario	I	II	III
Received mean power (dBm)	−33.0	−25.6	−18.9

2.2. Bit Error Rate for the Different Scenarios

In the previous subsection, the received power was computed considering the large scale fading only. In this subsection, the impact of multipath fading (small-scale fading) together with large-scale fading is also taken into account. Thus, the results of error analysis for the three communication scenarios simulated will be provided, as they were defined previously.

In modelling the small-scale variations of marine communication, the Extreme Value Distribution (EVD) will be used [3]. The EVD fits well with the experimental small-scale fading data when they are expressed in logarithmic scale. The EVD distribution is characterized by the location parameter, ν , and the scale parameter, ζ . Table 2 depicts the values of the small-scale fading parameters. The locations of the different nodes, with respect of the base station, are shown in Table 3.

Table 2. Values of data of the small-scale fading parameters.

Campaign	Location (ν)	Scale (ζ)
Base—Boat	0.164	1.45
Base—Buoy/UAV	0.164	1.45
Buoy/UAV—boat	0.160	1.35

Based on the parameters listed before, the error performance of the three communication scenarios was evaluated. Figure 4 shows that bit error rate (BER) significantly improves due to use of the UAV, as opposed to direct communication or buoy-based communication.

Table 3. Positions of different nodes of the simulations regarding base station.

Coordinates (m)	Base Station	Buoy	UAV
X	0	500	1000
Y	0	0	0
Z	9.8	1.9	185

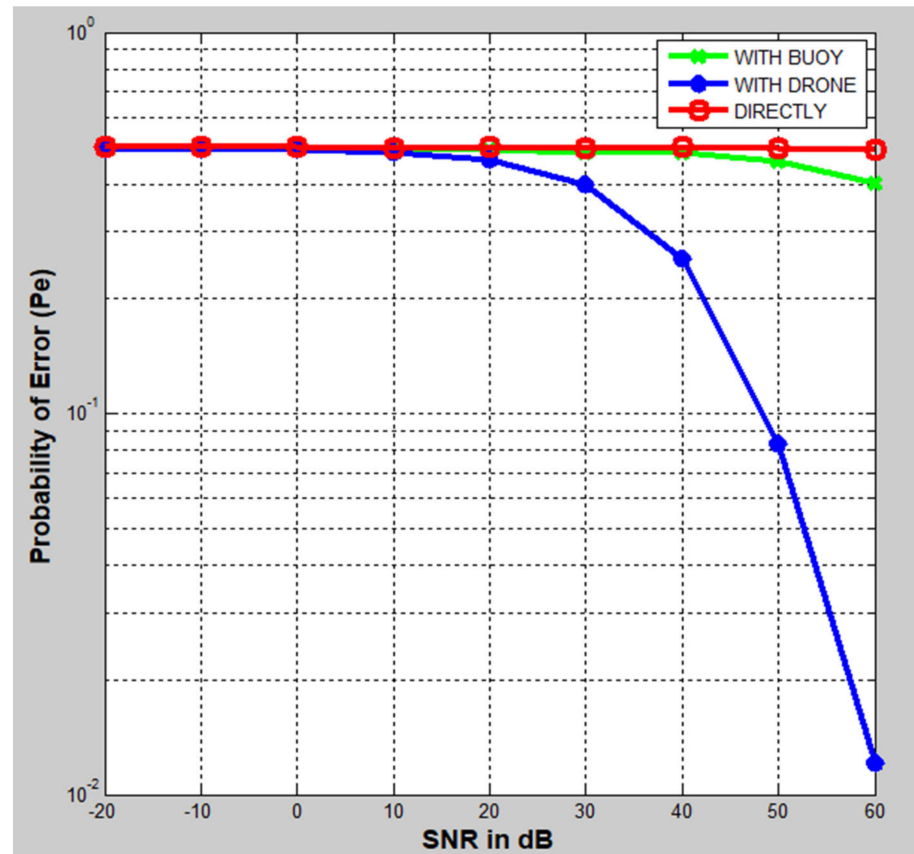


Figure 4. Comparison of signal loss directly, with buoy and with UAV.

As can be seen in Figure 4, the height greatly helps to reduce the probability of error, thus concluding that the UAV would be an excellent method to avoid the problems of marine communications. In the next section, the main objective of this paper will be started performing with the design, analysis and simulation of an array antenna patch with optimal transmission and matching characteristics.

3. Design of the Microstrip Antenna

The microstrip antennas [32–34] are going to become the source of connection between one point and another. For this reason, their study, design, and manufacture are going to be fundamental for the proper progress of marine communications, which are so difficult today.

3.1. Microstrip Line Feed

The power is supplied by microstrip line [32–35]. This method consists of connecting a microstrip line directly to the antenna, which is designed to possess the desired characteristic impedance. This type of power supply was chosen for several reasons: it is the simplest to feed, the manufacturing of antennas for different tests are more feasible, and the cost of this type of feed is minimal, compared to others.

3.2. Flexible Substrate

The substrate is the dielectric material on which the patch is placed and acts as an insulator, as well as directly influences the performance of the antenna.

One of the most important characteristics of the substrate is that it must be flexible, because the antenna will be positioned around the body of the UAV to radiate 360 degrees. The antenna will therefore have a cylindrical shape to cover all angles of radiation. Additionally, to reduce price of the antenna, it will be created in a 3D printer. Figure 5 shows an antenna on a curved substrate.

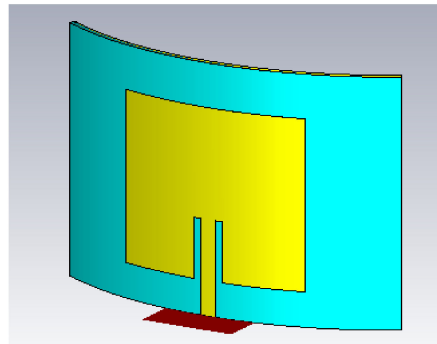


Figure 5. Patch antenna with a flexible substrate.

In the bibliography, several articles that explain their experiences with different flexible substrates manufactured in a 3D printer can be found;

In [11], the design of a Bowtie antenna with a PET (Polyethylene terephthalate) substrate, to improve wider bandwidth, at a frequency of 4.35 GHz.

In [12], the design of a circular patch antenna, made with an ABS (Acrylonitrile–Butadiene–Styrene) substrate in a 3D printer, at a frequency of 2.34 GHz, proving that ABS, even being a flexible material, shows better results than FR-4, which is the typical substrate used.

In [13], a 3D antenna is designed with NinjaFlex filament, to show its potential for RF circuits.

In [14], a study is made with different percentages of infill, different substrates, and different types of PLA antennas, concluding that the lower the percentage of infill the losses are higher at a frequency of 4 GHz.

In [15], a microstrip patch antenna operating at 38 GHz is designed to affirm the advantages of flexible substrate antennas over others, and its low cost and ease of fabrication is well documented. A comparison of different experiments that have been performed with different antennas, frequencies, and flexible substrates is found.

In [16], a microstrip patch antenna is designed with two substrates: ABS and NinjaFlex, which is flexible. The resonant frequency achieved is 2.305 GHz with a bandwidth of 0.12 GHz (5.21%), and when the antenna is flexed downwards, the resonant frequency shifts slightly upwards to 2.365 GHz (60 MHz) and the bandwidth is 0.13 GHz (5.71%).

In [17], a series of planar antennas on textile substrate and fed by a microstrip transmission line were designed and constructed, comparing their performance at different frequencies between 2 to 10 GHz.

The design of patch antennas on flexible substrates for radio frequencies must take into account two main parameters such as the dielectric constant and the tangent loss; however, the thickness is also very important. Increasing the thickness results in better radiation efficiency in the antenna, higher losses in the dielectric, and an increase in surface waves.

Knowing the arrangement of the antenna around the body of the UAV, it has been taken into account that the thinner the substrate is, the lighter the UAV will be, thus increasing the durability of the suspended UAV.

We have also taken into account the procurement, manufacture, and cost of the substrate; thus, for ease of design, rapid production, and minimum expense, we chose a material that could be manufactured with a 3D printer.

Finally, two parameters that have an important role in the choice of substrate were taken into account: the dielectric constant and the loss tangent, the former being the influence produced by an electric field on a material, while the latter quantifies the loss of signal due to the dissipation of electromagnetic energy from the substrate.

Different substrates have been compared in the following table, to check the most important characteristics for our study. These characteristics are that the substrate can be manufactured with a 3D printer, low cost, a flexible substrate, and the two constraints of dielectric constant and loss tangent, which must be met, to improve the antenna performance.

In the Table 4, a comparison between different substrates can be checked, checking the different characteristics related to the project. In the comparison, the PETG (Polyethylene terephthalate glycol) substrate stands out, which is the combination of PET with glycol, improving the interesting properties of PET with a glycolisation process, and it will be the one used to carry out the tests and check its effectiveness. The calculations from now on will be made knowing the dielectric constant and the loss tangent of the chosen substrate, PETG, which are 3 and 0.008, respectively.

Table 4. Advantages and disadvantages of different flexible substrates.

Substrate	Print 3D	Cost	Flexible	$1 \leq \epsilon_r \leq 5$	$\text{tang}(\delta) < 0.002$
TPU	Yes	Medium	High	4	0.04
Nylon	No	Medium	High	3.4	0.02
LCP	No	High	Medium	3.14	0.002
Ninjaflex	Yes	Medium	High	2.98	0.06
Teflon	No	Medium	Medium	2.1	0.002
PETG	Yes	Low	High	3	0.008
RO4003C	No	Medium	Low	3.38	0.0027

3.3. Impedance Matching or Coupling

Matching networks [35,36] avoid reflections generated on transmission lines due to the difference between the load impedance and the characteristic impedance, i.e., a matching network allows the input impedance of the network to match the impedance of the line so that the reflection coefficient is zero. The main advantages are optimizing the power delivered to the load, optimizing power losses in the supply line, and improving the signal-to-noise ratio of the system in receivers and transmitters.

The most common methods to implement the matching network are discrete elements, lambda/4 transformers, matching stubs, or a combination of them.

In this paper, two methods to implement the matching network will be discussed, and they are used for a microstrip antenna as well: lambda/4 transformer or InsetFeed [35,37].

In the bibliography, a multitude of papers can be found that study a microstrip antenna or array with different designs, substrates, and frequencies, and with them, we check and compare their conclusions and the results obtained.

In [18], a microstrip array design, with frequency of 5.4 GHz and substrate of FR4, RO4003C and ROGERS, is designed for use in a biostatic synthetic aperture radar. The types of feed networks are compared, and finally, a parallel feed of several antenna arrays is realised.

In [19], the design and simulation of rectangular microstrip antenna arrays (1, 2 × 1 and 4 × 1) for improved gain is presented. The substrate is ROGERS with thickness = 1.6 mm and the frequency of 2.4 GHz and the simulation is realised with HFSS (High Frequency Simulation Software). The gain of the three configurations is compared and it is checked that the bigger gain is the array of 4 × 1, which is 10.29 dB.

In [20], a fed rectangular microstrip patch antenna array (E-Shape) of 4 × 1 antennas is designed and fabricated. The resonant frequency from 1.9 GHz and the substrate ROGERS

RT Duroid with thickness 1.574 mm. The gain of the three configurations is compared and it is checked that the bigger gain is the array of 4×1 , which is 11 dB.

In [21], the experiences in the study and development of a microstrip dipole for the 2.4 GHz band and RF-35 substrate of 1.52 mm thickness is described. The results obtained are not optimal.

In [22], different microstrip antenna arrays of 5.8 GHz frequency and 1.5-mm thick DiClad 880 substrate are designed and simulated in HFSS, achieving a wide bandwidth and high gain.

In [23], two-dimensional 2×2 and 4×4 microstrip antenna arrays with $\lambda/4$ transformers are designed at a frequency of 9.5 GHz with the 0.508-mm thick Rogers RO4350 substrate, achieving a gain of 11.38 dBi and 17.32 dBi respectively. Improving the design and radiation characteristics, reducing the cost of the array.

In [24], a microstrip antenna is designed with a $\lambda/4$ transformer, an impedance of 75Ω for a frequency of 700 MHz and a 1.6-mm thick FR4 substrate, achieving a directivity of 7.4 dBi.

In [25], two microstrip antennas were designed and simulated with the HFSS and FEKO software, comparing the results with Rogers and FR4 substrate of 2 mm thickness. The square antenna was found to be more efficient at 3.5 GHz, while the circular antenna was more efficient at 6 GHz, both with FR4 substrate. The antennas achieved a directivity of 7.14 dB and 6.99 dB, respectively.

In [26], a patch antenna array (2×2) is designed at 2.44 GHz for WIFI and WIMAX applications and 1.5 mm thick Rogers RT5880 substrate, achieving a directivity of 13.42 dBi with high radiation efficiency.

In [27], a patch antenna of frequency 5.4 GHz is designed and simulated in IE3D software, and real tests are performed with a Vector Analyser. The chosen substrate was Bakelite and a thickness of 1.6 mm, reaching a gain of 5.42 dB, proving that there are differences between simulation and reality, as there are many factors that are not taken into account in the simulation.

In [28], a patch antenna array of frequency 60 GHz is designed to achieve a directivity of 21 dBi. This parameter was achieved with 6 arrays in parallel and each with 6 arrays in series, on a 0.254-mm thick Rogers 5880 substrate.

In [29], it is desired to design, simulate, and build an array of patch antennas at a frequency of 740 MHz, with the FR4 substrate and thickness 1.5748 mm, meeting gain (5–6 dBi) and bandwidth (690–790 MHz) characteristics being the most relevant.

In [30], a microstrip antenna and a 2×2 array at a frequency of 10.5 GHz, with FR-4 substrate of 1.5 mm thickness, are designed, simulated, fabricated, and analysed. The array achieves a gain of 9.26 dBi.

3.3.1. Coupling and Feeding with a Quarter Wavelength Transmission Line

In the case of a quarter lambda transformer coupling network, the variation in the position of the microstrip line relative to the patch will generate a higher or better impedance coupling. The microstrip antenna can be matched to a transmission line of characteristic impedance (Z_0) by a transmission line of quarter wavelength impedance (Z_c) [38]. Microstrip feed with a quarter wavelength transmission line is shown in Figure 6, while microstrip feed with InsetFeed is shown in Figure 7.

To achieve impedance matching where the input impedance $Z_{in} = Z_0$, and the antenna impedance Z_L , requires that:

$$Z_0 = \frac{Z_c^2}{Z_L}, \quad (3)$$

The Z_c parameter can be altered by changing the width of the quarter-wavelength strip. The wider the matching line, the lower the characteristic impedance (Z_0).

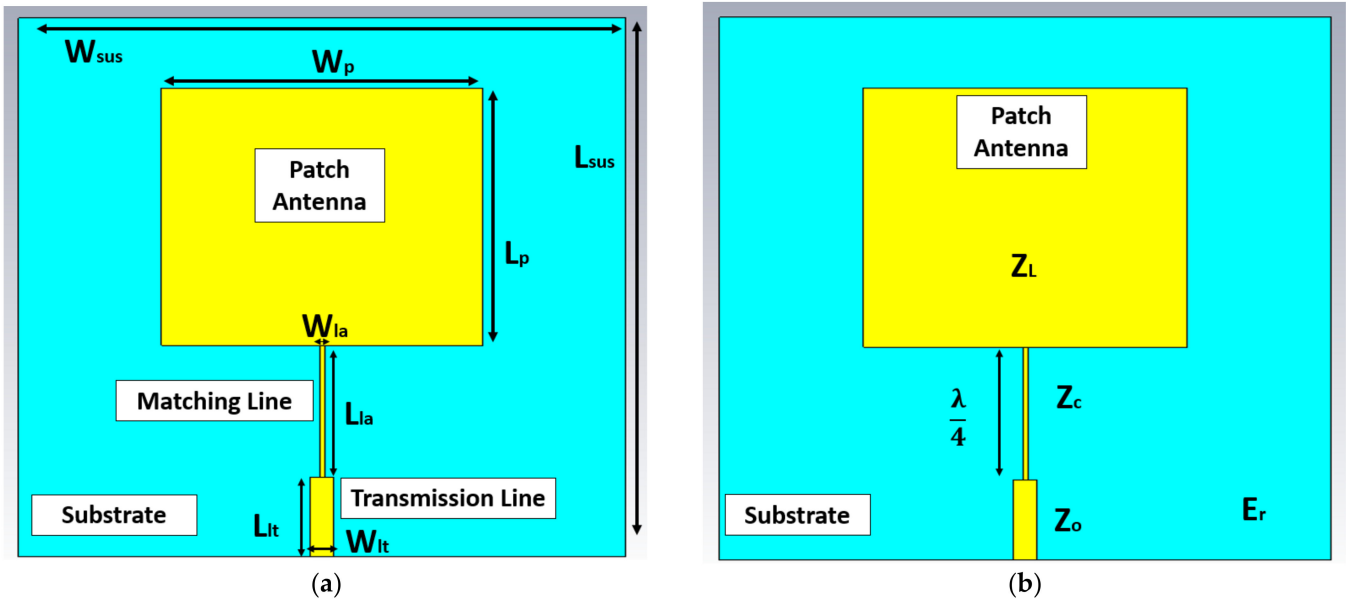


Figure 6. Both figures are microstrip feed with a quarter wavelength transmission line. (a) details of the sizing parameters, and (b) impedances.

3.3.2. Coupling and Feeding with InsetFeed

In the case of insertion feeding, it is the depth of the insertion that dictates the impedance coupling. With this insertion, since the current is low at the ends of a half-wave patch and increases in magnitude towards the centre, the input impedance is reduced as the patch is fed closer to the centre [38].

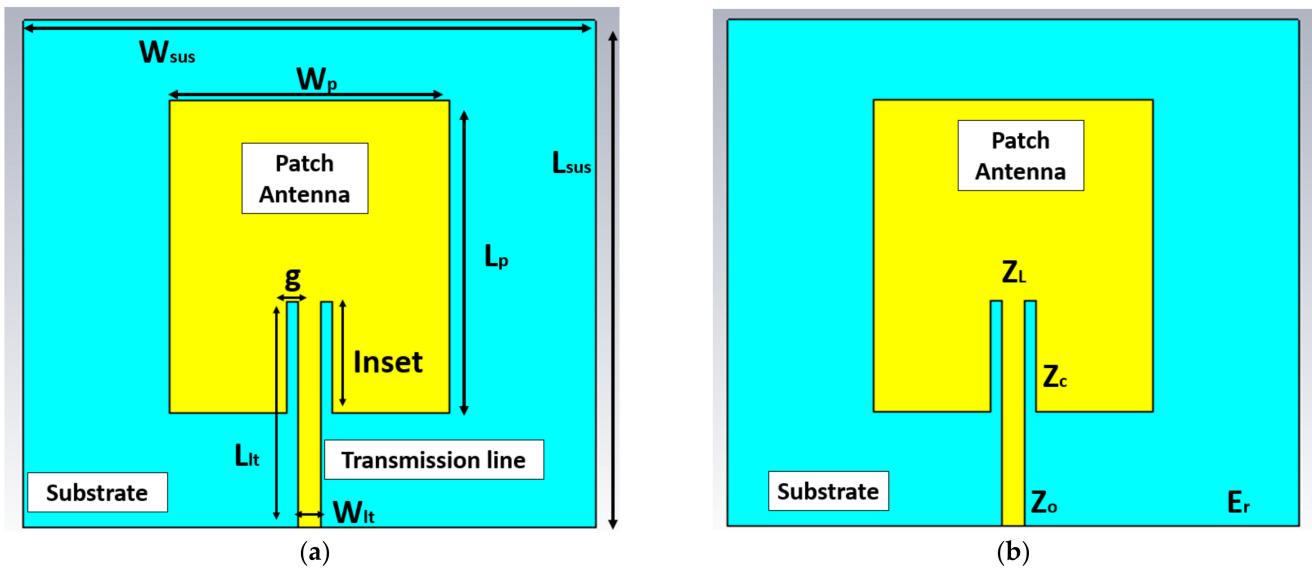


Figure 7. Both figures are microstrip feed with InsetFeed. (a) details of the sizing parameters, and (b) impedances.

To achieve an impedance match the input impedance $Z_{in} = Z_o$, and the antenna impedance Z_L , it is required that:

$$Z_o(R) = \cos^2 \left(\frac{Z_c^2}{Z_L} \right) \times Z_o(0) \tag{4}$$

By varying the distance R, a parameter that can be seen in the figure above, the voltage-current relationship will not be so high, achieving characteristic impedance values similar to those of the microstrip line. As can be seen in the image, the most representative difference between the InsetFeed adaptation and the fourth lambda transformer is a notch of length R at the input of the patch, which introduces a capacitive component modifying the resonance frequency of the patch.

In this paper, a study of both feeds and adaptations will be carried out to determine the preferable option to be introduced into the system in two different frequencies: 2.4 GHz and 5.2 GHz.

3.4. Patch Antenna Design Calculations

In this subsection, the sizing of four different rectangular patch antennas is going to be calculated depending on their frequency (2.4 GHz and 5.2 GHz), and their feeding and coupling method (fourth lambda transformer or InsetFeed), for their subsequent study in simulation.

These four antennas will be dimensioned and simulated for the same previously defined substrate, PETG, with a dielectric constant of value 3 and a loss tangent of value 0.008.

Next, the calculation of the substrate thickness, h, will be carried out, which will be determined by [32],

$$0.005\lambda \geq h \geq 0.2\lambda, \tag{5}$$

The following subsection describes the transmission line model, useful for thin substrates $\left(\frac{h}{\lambda_0} < \frac{1}{100}\right)$ with respect to the wavelength in free space of the signal at which the antenna in question will resonate.

A description of the design procedure for rectangular microstrip antennas is given below. The procedure assumes that the specified information includes the dielectric constant of the substrate ($\epsilon_r = 3$), the resonant frequency (that is in GHz = 2.4 GHz or 5.2 GHz), the characteristic impedance ($Z_0 = 50 \Omega$) and the thickness of the substrate. The procedure is as follows:

First of all, let us calculate the wavelength at a frequency 2.4 GHz and 5.2 GHz, respectively, with the equation, $\lambda_0 = \frac{c}{f}$:

$$\lambda_0 = \frac{3 \times 10^8}{2.4 \times 10^9} = 125 \text{ mm} \tag{6}$$

$$\lambda_0 = \frac{3 \times 10^8}{5.2 \times 10^9} = 57.7 \text{ mm} \tag{7}$$

Knowing the wavelengths of both frequencies, it is important to determine the thickness of the substrate (h):

$$\frac{h}{\lambda_0} < \frac{1}{100} \text{ so } h \text{ must be } < \frac{\lambda_0}{100} \tag{8}$$

Thus, $h < 1.25 \text{ mm}$ if Fr is 2.4 GHz and $h < 0.577 \text{ mm}$ if Fr is 5.2 GHz.

For an antenna with good radiation efficiency, its width (W) is determined by the following equation, which is based on radiation efficiency criteria studied by Bal and Bhartia:

$$W = \frac{c_0}{2f} \sqrt{\frac{2}{(\epsilon_r + 1)}}, \tag{9}$$

where c_0 is the speed of light, fr is the frequency at which we work, and ϵ_r is the dielectric constant of the chosen substrate.

The length of the patch can be determined by the solution of the next equation:

$$L = \frac{c_0}{2f \times \sqrt{\epsilon_{eff}}} - (2 \times \Delta l) \tag{10}$$

where E_{eff} is the effective dielectric constant of the microstrip antenna, which is calculated by the following null equation:

$$E_{\text{eff}} = \frac{e_r + 1}{2} + \left(\frac{e_r - 1}{2} \right) \left(1 + \frac{12 \times h}{W} \right)^{-0.5} \tag{11}$$

And Δl is the length increment that was calculated,

$$\Delta l = 0.412 h \times \frac{(E_{\text{eff}} + 0.3) \times \left(\frac{W}{h} + 0.264 \right)}{(E_{\text{eff}} - 0.258) \times \left(\frac{W}{h} + 0.8 \right)} \tag{12}$$

Typical microstrip patch lengths are given by equation,

$$L \approx (0.47 - 0.49) \frac{\lambda_0}{\sqrt{e_r}} = (0.47 - 0.49) \lambda \tag{13}$$

where λ is the wavelength in the dielectric

$$\lambda = \frac{\lambda_0}{\sqrt{e_r}} \tag{14}$$

The next step would be to calculate the transmission line length and width.

$$L_{\text{LT}} = \frac{\lambda}{4}, \tag{15}$$

where L_{LT} is the length of the transmission line and the W_{LT} is the width of the transmission line:

$$W_{\text{LT}} = \frac{8he^A}{e^{2A} - 2} \text{ if } \frac{W_{\text{LT}}}{h} < 2 \tag{16}$$

Or

$$W_{\text{LT}} = \frac{2h}{\pi} \left[B - 1 - \ln(2B - 1) + \frac{e_r - 1}{2e_r} \ln(B - 1) + 0.39 - \frac{0.61}{e_r} \right] \text{ if } \frac{W_{\text{LT}}}{h} > 2 \tag{17}$$

where B and A are variables that can be calculated with the following equations:

$$B = \frac{377\pi}{2Z_0(\sqrt{e_r})} \text{ and } A = \left(\frac{Z_0}{60} \right) \times \left(\frac{e_r + 1}{2} \right)^{0.5} + \left(\frac{e_r - 1}{e_r + 1} \right) \times \left(0.23 + \frac{0.11}{e_r} \right) \tag{18}$$

The length and width of the substrate is determined:

$$W_{\text{susmin}} = 6h + W \tag{19}$$

$$L_{\text{susmin}} = 6h + L \tag{20}$$

where W_{susmin} and L_{susmin} are the minimum width and length to be assigned to the substrate, respectively.

The impedance of the antenna can be calculated as indicated in the following equation:

$$R_{\text{in}} = \frac{1}{2G_1 \pm G_{12}} \tag{21}$$

where R_{in} is the actual impedance of the antenna expressed in ohms, G_1 and G_{12} are the conductance at the input resistance, and are calculated below:

The InsetFeed patch antenna, as has been seen previously, has two radiation spaces, therefore, the total admittance in slot #1 (input admittance) is obtained by transferring

the admittance of slot #2 from the output terminals to the input terminals. Solving, it is obtained that the total resonant input admittance is real and is given by:

$$Y_{in} = Y_1 + Y_{12} = 2G_1 \tag{22}$$

Knowing that the input impedance will then be:

$$Z_{in} = \frac{1}{Y_{in}} = R_{in} = \frac{1}{2G_1} \tag{23}$$

where G_1 can be expressed as follows:

$$G_1 = \frac{I_1}{120\pi^2} \tag{24}$$

$$I_1 = \int_0^\pi \left[\frac{\text{sen}\left(\frac{K_0W}{2} \cos(\theta)\right)}{\cos(\theta)} \right]^2 \text{sen}^3(\theta) d\theta = -2 + \cos(X) + X_s(X) + \frac{\text{sen}(X)}{X} \tag{25}$$

where:

$$X = K_0W \tag{26}$$

And K_0 is the phase constant, being:

$$K_0 = \frac{2\pi}{\lambda} \tag{27}$$

The resonant input resistance, given by the above equation, does not take into account the mutual effects between the slots. Making such a consideration, the equation number is obtained, the mutual conductance G_{12} can be calculated as follows, where J_0 is the first-species zero-order Bessel function:

$$G_{12} = \frac{1}{120\pi^2} \int_0^\pi \left[\frac{\text{sen}\left(\frac{K_0W}{2} \cos(\theta)\right)}{\cos(\theta)} \right]^2 J_0(K_0L\text{sen}(\theta)) \text{sen}^3(\theta) d\theta \tag{28}$$

With this data, the distance of the insertion point, called inset in this project, can be calculated:

$$y_0 = \frac{L}{\pi} \times \cos^{-1} \left(\sqrt{\frac{Z_0}{R_{in}}} \right) \tag{29}$$

The next factor to determine is the separation distance between the patch and the feed line. This is determined with the equation:

$$g = \frac{c}{\sqrt{2E_{eff}}} \frac{4.65^{-12}}{f[\text{Ghz}]} \tag{30}$$

For a patch antenna with a fourth lambda transformer feed, the calculation of the patch is exactly the same. However, the calculation of y_0 and g is not necessary, and the calculation of the impedance of the transmission line and the antenna is also different. R_{in} calculates it in the program, using the above equations. The results are shown in Table 5.

Table 5. Calculation of antenna parameters depending on feed type and frequency.

Feeding	F_r	λ_o	λ	W_p	L_p	L_{ia}	W_{ia}	Y_o	g	W_{LT}	L_{LT}
InsetFeed	2.4	125	72.17	44.2	36	-	-	12.9	1.38	1.30	18.04
	5.2	57.7	33.31	20.40	16.51	-	-	5.91	3.02	1.30	8.33
$\lambda/4$	2.4	125	72.17	44.2	36	18.04	0.22	-	-	1.3	5
	5.2	57.7	33.31	20.40	16.51	8.33	0.22	-	-	1.3	5

3.5. Patch Antenna Simulation

In this subsection, the performance of the antennas calculated in the previous subsection will be designed and simulated. The program chosen is CST Studio Suite because of its speed in simulation, its low RAM consumption, and its features to achieve the design required to simulate. The steps to carry it out are detailed below:

Firstly, the workflow for the project is detailed: MW and RF and Optical, and Antennas is selected, and finally, the type of Antenna: Patch.

Then, the program makes it possible to choose the type of domain, for this project, the Tempo Domain, and the maximum and minimum simulation frequency is chosen.

After creating the simulation environment, the antenna design is carried out. The design process is divided into three layers: the PETG substrate layer of $h = 0.5$ mm, the copper ground plane which is underneath the substrate, and its thickness depends on the prototyping machine used, $h = 0.025$ mm, and the patch antenna created above the substrate and h than the ground plane.

In the following Figure 8 show (a) the patterning of the substrate in light blue, which represents PETG, (b) the ground plane in yellow, representing Cu, and (c) patch antenna in yellow. The width of the transmission line is calculated in Figure 9.

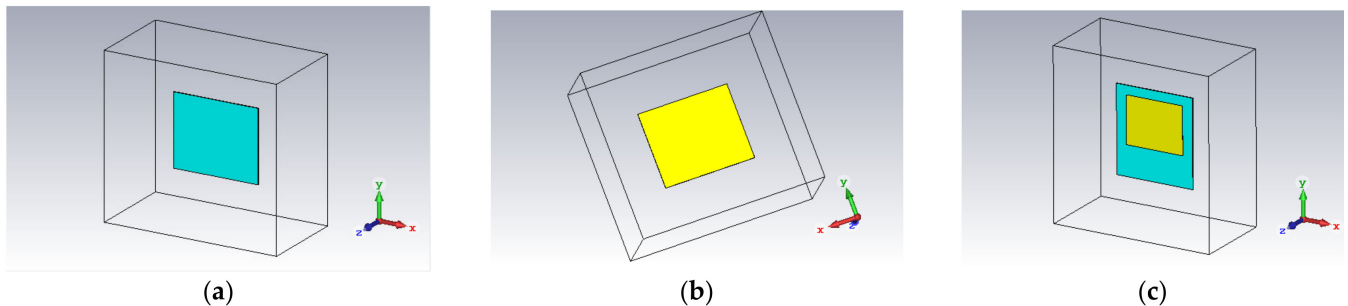


Figure 8. (a) Substrate, (b) ground, and (c) patch antenna.

The antenna layer is made, which includes the body of the patch antenna, the $\lambda/4$ transformer matching line and the 50Ω impedance transmission line.

In the design calculations, the width of the transmission line was calculated with impedance $Z_0 = 50 \Omega$. However, the matching line has an impedance of $Z_c = 117 \Omega$, which is essential for the width calculation. The length, as we know, is calculated as $\lambda/4$, while the width can be calculated by various applications. CST program allows us, through a MACRO, "Impedance Calculation", to calculate the width by adding the data required for the calculation, as can be seen in the following figure.

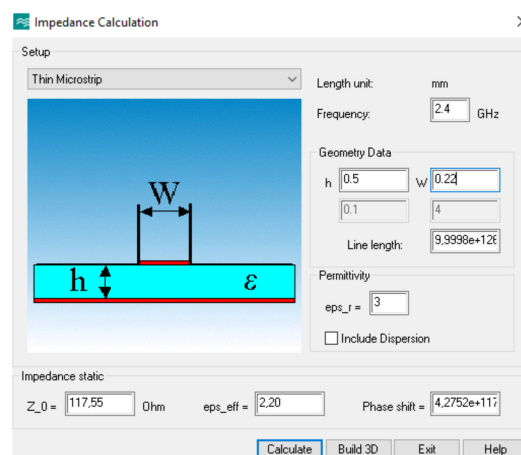


Figure 9. Calculation of the width of the transmission line (W_{la}) knowing the antenna impedance.

The fixed value of h is added, frequency, dielectric constant and W , the latter is the one that that can be modified, and then, “Calculate” must be pressed, to calculate the impedance Z . The calculation method is trial and error, until the result is $Z = 117$, or as close as possible. $W = 0.22$ mm, $Z = 117.55$ Ω .

Note that the impedance matching in the InsetFeed patch is performed through the I -value, calculated in Equation (25). However, for the $\lambda/4$ transformer patch, it is calculated by performing a calculation between the input impedance and the antenna impedance. The antenna impedance depends on the values of W_p (patch width) and L_p (path length). When these are modified, consequently, the antenna impedance changes and, in turn, the impedance of the matching line, having, in turn, a new value of matching line width.

Finally, the transmission line is added, being the length of the transmission line indifferent while the width was calculated for $Z_o = 50$ Ω , where $W_{LT} = 1.3$ mm. The next figures show the steps for antenna design.

Before starting the simulation, a power supply port at the end of the transmission line must be created (see in Figure 10). This is calculated with a MACRO called “Calculate Port Extension Coefficient” and, by indicating the position where the port will be located, it calculates and paints it directly, as shown in the following image.

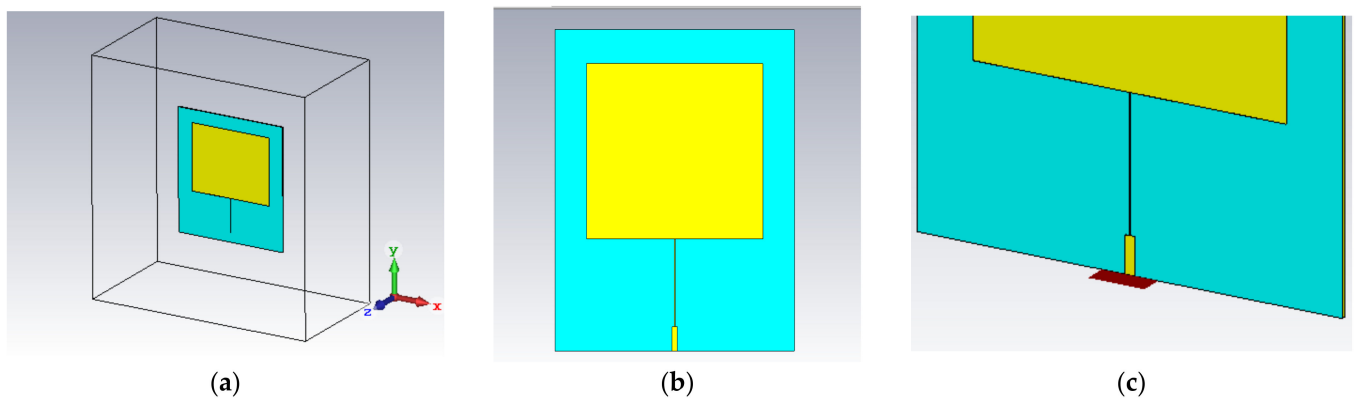


Figure 10. (a) Transmission line, (b) design of the patch antenna, and (c) power supply.

Next, press the “Start Simulation” button to start calculating the different parameters needed to evaluate if the antenna is correctly designed, such as S_{11} , VSWR, impedance matching (Z), Gain, and Directivity.

The Figure 11 shows the value of parameter S_{11} . In which, it can be seen how, at the 2.4 GHz value, which is the resonance frequency value, the power in decibels of the signal is almost zero (-1.688 dB), i.e., almost all the signal power sent is returned (it does not resonate). Moreover, being its highest power at the 2.36 GHz frequency, it is very low (-8.6 dB).

The Figure 12 shows the matching of the reference impedance. In the project, a reference impedance of 50 Ω was determined. However, the result of the simulation gives an impedance of 47.48 Ω .

The Figure 13 shows the standing wave voltage ratio, a measure of the efficiency with which RF energy is transmitted from the power source through the transmission line to the antenna patch, is tested. A value of less than 2 is considered adequate; however, the result was 10.32.

Finally, the Figure 14 shows the directivity values on the left, 6.91 dBi, and gain on the right, 2.21 dB, are obtained. These values are optimal for an antenna of this type. However, the values of the S_{11} parameter, the reference impedance and VSRM are not optimal for the antenna design. The adaptation is deficient, this is due to the fact that the equations give results with so many decimal numbers accumulating errors, and in addition, the PCB printing machine of our laboratory has a minimum printing scale of 0.02 mm.

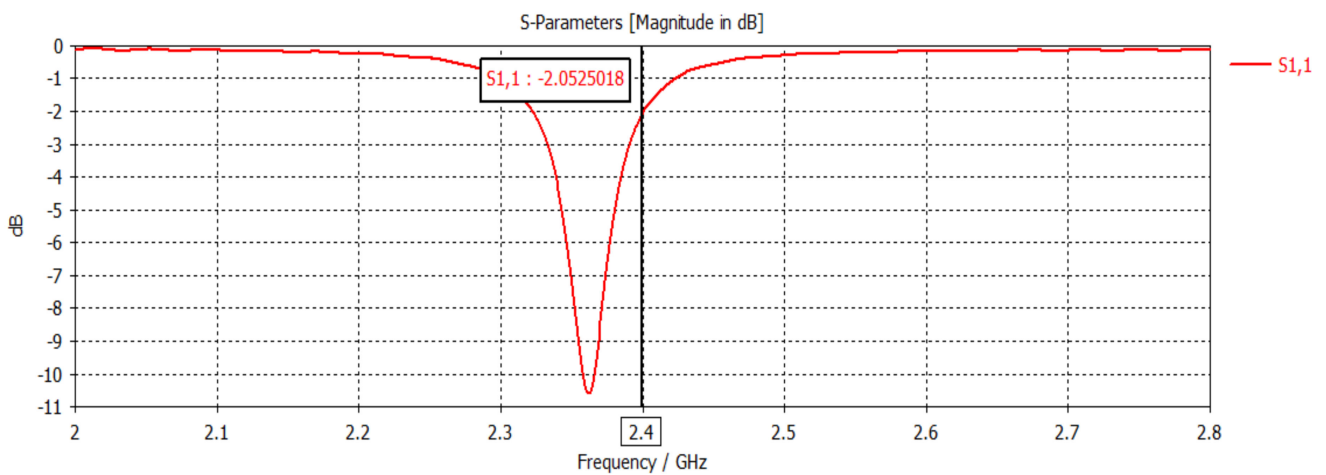


Figure 11. S₁₁ parameter by frequency in patch antenna of 2.4 GHz with line transmission $\lambda/4$.

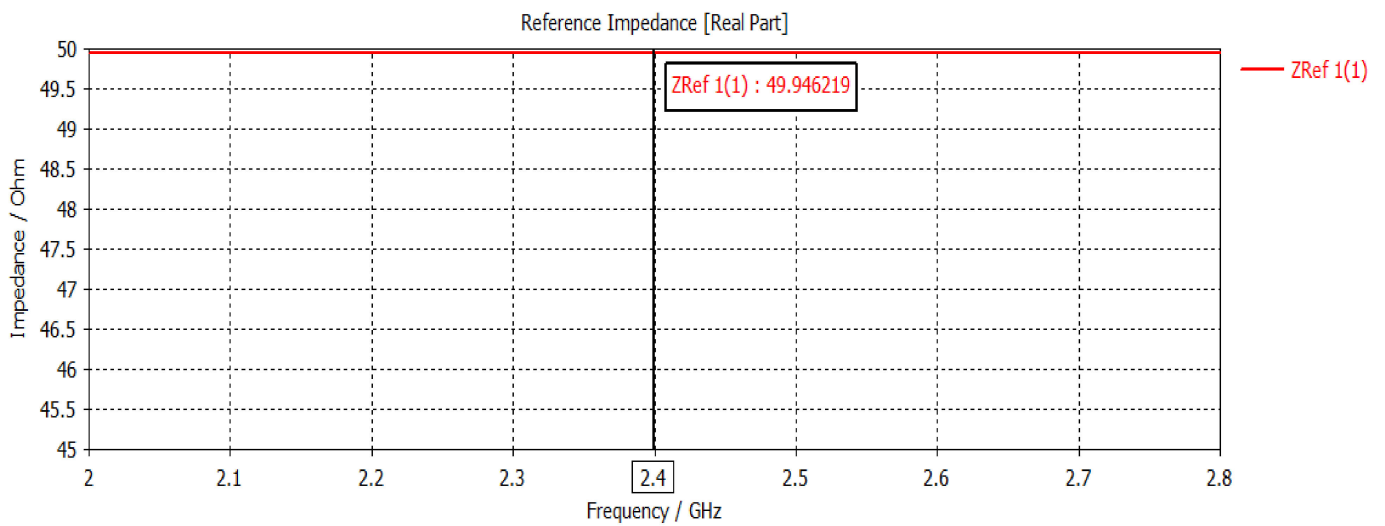


Figure 12. Impedance by frequency in patch antenna of 2.4 GHz with line transmission $\lambda/4$.

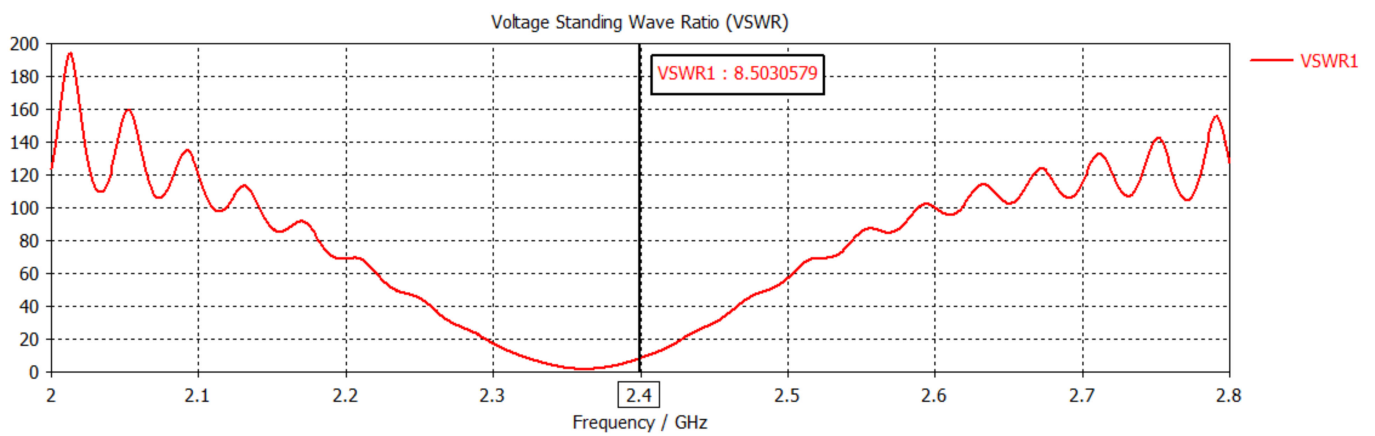


Figure 13. VSWR by frequency in patch antenna of 2.4 GHz with line transmission $\lambda/4$.

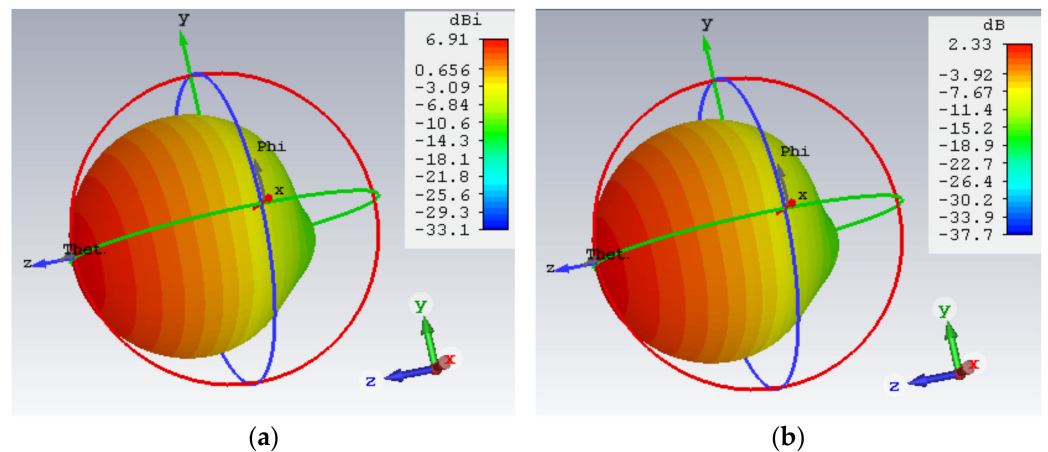


Figure 14. (a) Directivity and (b) gain (right) of patch antenna of 2.4 GHz with line transmission $\lambda/4$.

For this reason, a study is made in this paper, about how the values of the parameters calculated in the equations vary according to the parameters introduced by simulation, to get optimal results in transmission and matching. This study was carried out by the trial-and-error method, introducing higher and lower values of the antenna input parameters in the simulation and checking the variation of the output calculations.

The results of various simulations of both the $\lambda/4$ transformer antenna (the following table) and the InsetFeed antenna can be seen below. In the left column, the antenna parameters to be modified are shown and the effect of increasing or decreasing their value is checked. The first row describes the main parameters taken into account for this study, which can go up, down, or not change their value (=). In addition to these fixed values, some values vary depending (unclear) on how much the input value is increased or decreased. The results of the simulation the $\lambda/4$ antenna with different input parameters are shown in Table 6.

Table 6. Result of the study of simulating the $\lambda/4$ antenna with different input parameters.

Outputs		S11	BW	Directivity	Z	VSWR	Gain
Inputs							
W_p	UP	↓	↓	↑	=	Unclear	↑
	DOWN	↑	↑	↓	=	Unclear	↓
L_p	UP	↓	↑	↑	=	=	↓
	DOWN	↑	↓	↓	=	=	↑
L_{1a}	UP	=	Unclear	↑	=	=	↓
	DOWN	=	Unclear	↓	=	=	↑
W_{1a}	UP	=	Unclear	=	↓	=	=
	DOWN	=	Unclear	=	↑	=	=
L_{LT}	UP	=	↓	=	=	↑	↑
	DOWN	=	↓	=	=	↑	↓
W_{LT}	UP	↑	↓	↑	Unclear	↑	↓
	DOWN	↓	↓	↓	Unclear	↓	↑

The same tests were carried out for an InsetFeed antenna as with the $\lambda/4$ antenna, and the results obtained are shown in Table 7.

Table 7. Result of the study of simulating the InsetFeed antenna with different input parameters.

Outputs		S11	BW	Directivity	Z	VSWR	Gain
Inputs							
W_p	UP	↓	↓	↑	=	Unclear	↑
	DOWN	↑	↑	↓	=	Unclear	↓
L_p	UP	↓	↑	↑	=	=	↓
	DOWN	↑	↓	↓	=	=	↑
L_{LT}	UP	=	=	↑	=	=	↓
	DOWN	=	=	↓	=	=	↑
W_{LT}	UP	=	=	=	↓	=	=
	DOWN	=	=	=	↑	=	=
INSET	UP	=	↓	=	=	↑	↑
	DOWN	=	↓	=	=	↑	↓
g	UP	↑	↓	↑	=	↑	↓
	DOWN	↓	↓	↓	=	↓	↑

In the previous tables, the parameters that have been modified are analysed. Thus, the results of the Outputs, ↑, ↓, =, Unclear, are calculated when the Inputs UP or DOWN. For instance, when the W_p , UP, the value of S11 down, but if the W_p , DOWN, the value of S11 UP. The Outputs = and UNCLEAR mean that the result does not change. In the Table 8, the meaning of abbreviations.

Table 8. Input and output parameters of the antennas.

Inputs	Outputs
W_p : width of the patch	S11: parameter S11
L_p : length of the patch	BW: bandwidth
W_{la} : width of the adaptation line	Directivity
L_{la} : length of the adaptation line	Z: impedance
L_{LT} : transmission line	VSWR: line in standing wave ratio
W_{LT} : width of the transmission line	Gain
W_{sus} : width of the substrate	
L_{sus} : length of the substrate	
g : separation distance between the patch and the feed line	
Y_o : Inset	
W_{in} : width of the feed line (only array)	
L_{in} : Length of the feed line (only array)	
Distance Array: distance between the center of the each patch antenna (only array)	

This study helps to design, fix, and achieve an appropriate and effective antenna, in order to obtain profitable radio link results.

Comparing the results obtained for the values of the parameters calculated in the equations and the values of the parameters obtained in the simulated antenna, we can see in the Figures 15–18 the difference in optimisation between them. The results of the first simulated antenna showed almost no matching, but higher directivity and gain, while in the case of the second simulated antenna, which was tested with many simulations, a little bit lower directivity and gain but a high matching were shown, which is what we were trying to achieve.

3.6. Results Obtained for a Microstrip Antenna

In this subsection, the results obtained from both antennas are assembled, and the results obtained from the equation calculations are compared with the best simulated result, taking into account all the values of the outputs (antenna output parameters), in the Table 9.

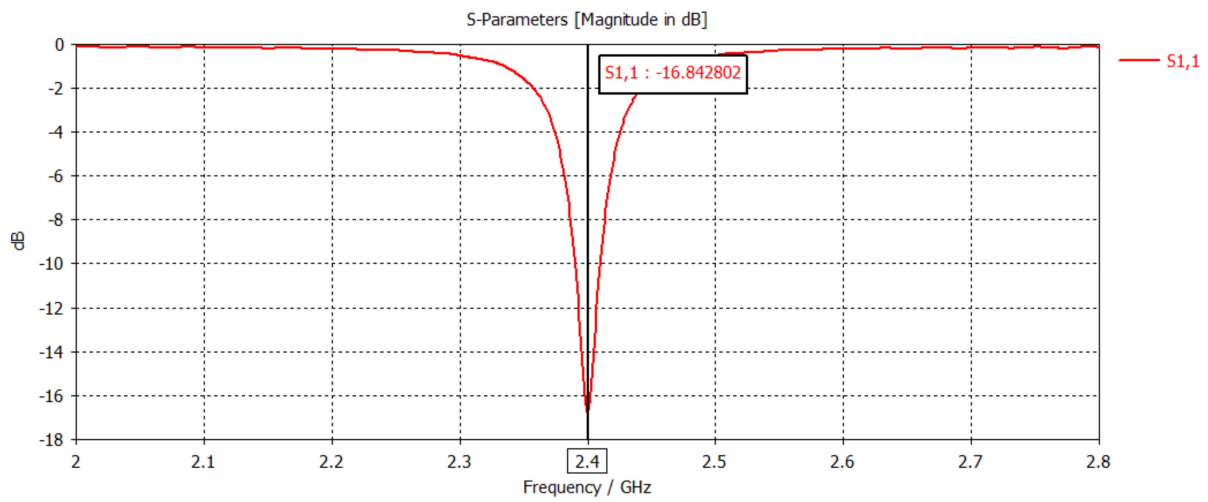


Figure 15. S11 parameter by frequency in new design of patch antenna of 2.4 GHz with line transmission $\lambda/4$.

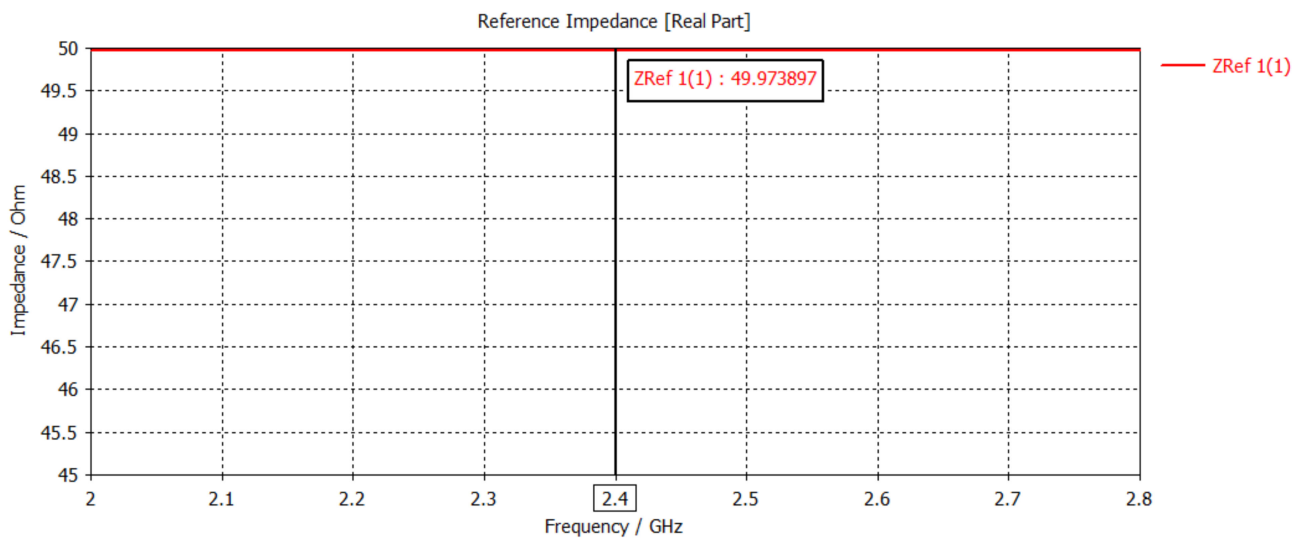


Figure 16. Impedance by frequency in new design of patch antenna of 2.4 GHz with line transmission $\lambda/4$.

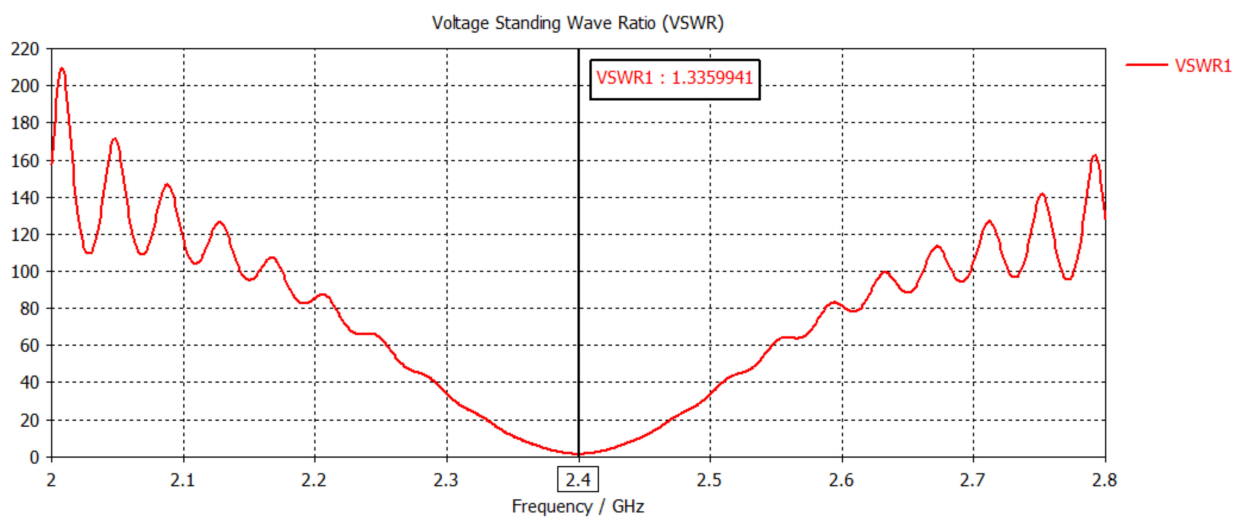


Figure 17. VSWR by frequency in new design of patch antenna of 2.4 GHz with line transmission $\lambda/4$.

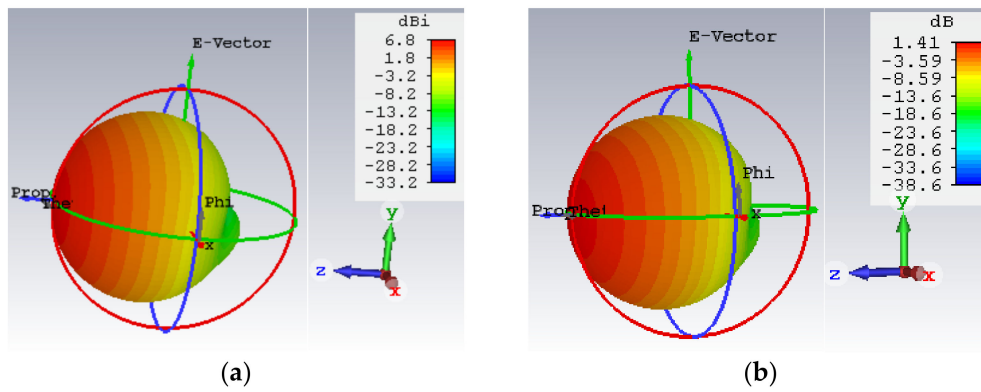


Figure 18. (a) Directivity and (b) gain (right) of new design of patch antenna of 2.4 GHz with line transmission $\lambda/4$.

Table 9. Inputs and outputs of the calculated and simulated parameters of the antennas.

	2.4 GHz $\lambda/4$		2.4 GHz Inset		5.2 GHz $\lambda/4$		5.2 GHz Inset	
	EQN	Simulation	EQN	Simulation	EQN	Simulation	EQN	Simulation
Inputs								
W_p (mm)	44.2	30	44.2	30	20.4	15.9	20.4	14.7
L_p (mm)	36	35.62	36	36	16.5	16.18	16.5	16.54
W_{la} (mm)	0.34	0.2	–	–	0.34	0.24	–	–
L_{la} (mm)	18.04	17	–	–	8.32	8.32	–	–
W_{LT} (mm)	1.2	1.2	1.3	1.22	1.2	1.18	1.3	1.22
L_{LT} (mm)	5	5	18.04	20	5	5	8.32	8.32
Y_o (mm)	–	–	12.9	11.5	–	–	5.9	5.9
g (mm)	–	–	1.38	0.6	–	–	3.02	0.6
W_{sus}	70	70	70	70	30	30	30	30
L_{sus}	61.5	61.5	61.5	61.5	23	23	23	23
Outputs								
S11 (dB)	–2.05	–17	–2.53	–32.29	–2.29	–24.51	–0.37	–25.25
BW (MHz)	0	20	0	25.6	0	65.1	0	74.5
Z (Ω)	49.95	49.97	47.89	49.87	49.38	49.87	49.81	49.86
VSWR	8.5	1.33	6.91	1.05	7.62	1.13	46	1.11
Directivity (dB)	6.91	6.8	7.2	7.06	7.12	6.97	7.05	6.64
Gain (dBi)	2.33	1.41	2.64	1.86	4.14	3.92	2.03	4.3

All the values are calculated directly from the CST Studio program, except the BW value is calculated by subtracting the lower and upper frequency from the cut-off frequency, which crosses with a value of -10 dB.

Observing the results obtained from the tests between the calculated and simulated antennas, it can be seen that the calculated antennas have a higher directivity. However, other important characteristics, such as matching and coupling, are very weak.

4. Design and Simulation of Patch Antenna Arrays

In this section, an array of previously verified patch antennas will be designed and simulated. Therefore, a study of four 2×1 arrays will be carried out in order to compare their results and determine which one is more effective for the project.

The following should be taken into account in order to make a correct adaptation between the different transmission lines:

1. Firstly, the impedance of the supply line is determined, which is equal to 50Ω .
2. Next, the transmission line is divided in two, so that the impedance becomes 100Ω .
3. The impedance of the antenna is calculated by the Equation (23).

- Finally, the impedance of the matching line is calculated by the root of the product of the antenna impedance times the 100Ω impedance.

As can be seen, there is a difference between the input impedance of the patch antenna, which was equal to 50Ω , while in the array the input impedance is 100Ω . This is due to the fact that in the array the feed line is split in two, which causes the input impedance to double from 50Ω to 100Ω .

In addition to the design shown in the previous image, where the input impedance of the array patch has been determined at 100Ω , a design with 50Ω could have been made, as in the previous section. However, an additional matching line would have to be added between the 50Ω input of the patch and the 100Ω of the power supply transmission line. This line would mean a higher occupancy, which is detrimental to the interests of weight and size of the UAV.

The following Figures 19 and 20 show the design and the calculated impedance in each transmission line. If both figures are compared, the difference between the impedances can be observed. As in Section 3, an analysis is made for the two types of patch antenna feeds, in order to achieve better antenna output characteristics. In contrast to the previous section, the analysis will be performed with a patch antenna array.

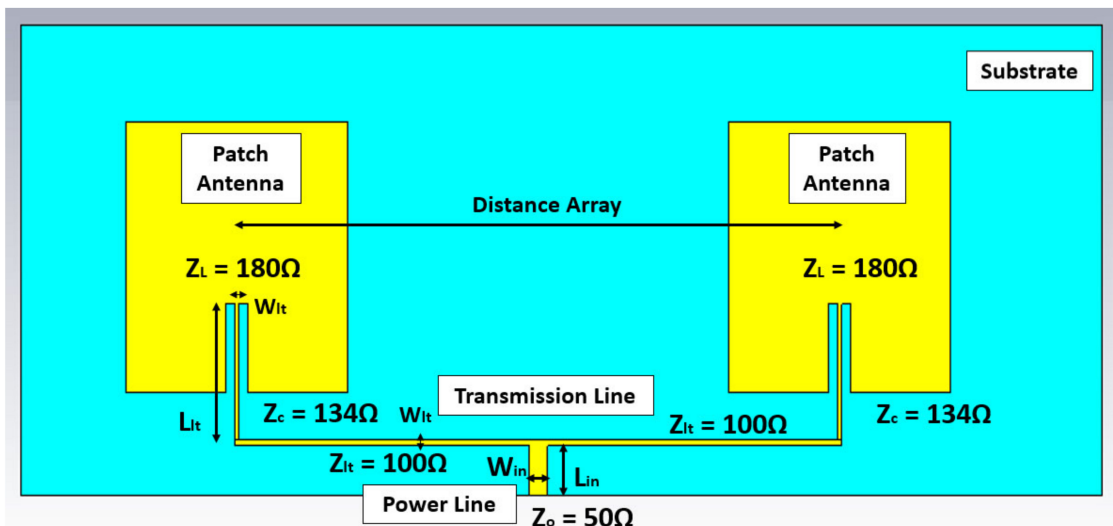


Figure 19. Design of the patch array antenna 2×1 and InsetFeed.

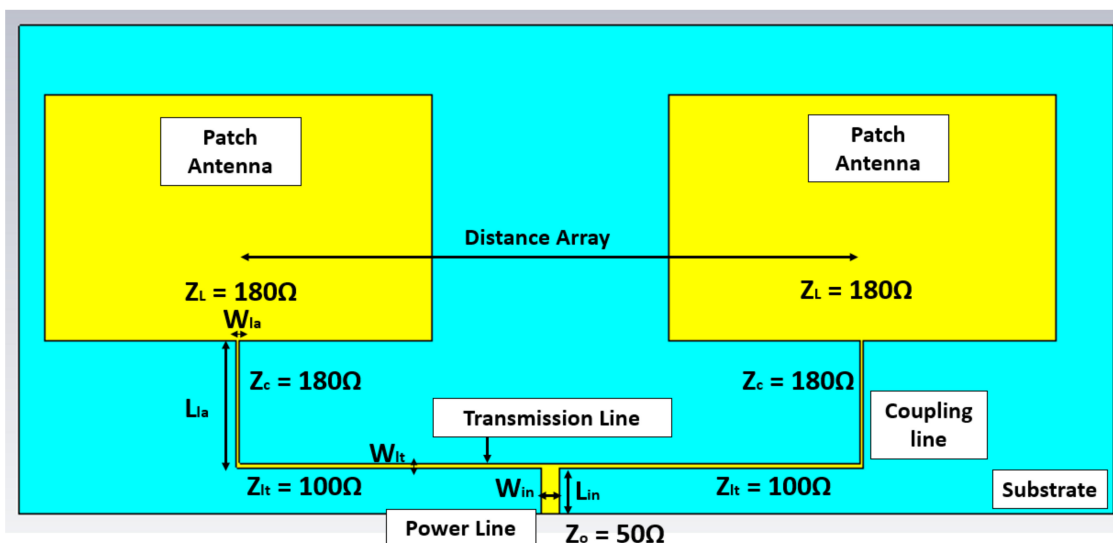


Figure 20. Design of the patch array antenna 2×1 and lambda quarter.

The results of the simulation the $\lambda/4$ antenna with different input parameters are shown in Table 10.

Table 10. Result of the study of simulating the $\lambda/4$ antenna with different input parameters.

Outputs		S11	BW	Directivity	Z	VSWR	Gain
Inputs							
W_p	UP	↓	↓	↑	=	Unclear	↑
	DOWN	↑	↑	↓	=	Unclear	↓
L_p	UP	↓	↑	↑	=	=	↓
	DOWN	↑	↓	↓	=	=	↑
L_{1a}	UP	=	Unclear	↑	=	=	↓
	DOWN	=	Unclear	↓	=	=	↑
W_{1a}	UP	=	Unclear	=	↓	=	=
	DOWN	=	Unclear	=	↑	=	=
L_{LT}	UP	=	↓	=	=	↑	↑
	DOWN	=	↓	=	=	↑	↓
W_{LT}	UP	↑	↓	↑	Unclear	↑	↓
	DOWN	↓	↓	↓	Unclear	↓	↑
Distance Array	UP	↑	=	↑	=	↑	↑
	DOWN	↓	↓	↓	=	↑	↓
W_{in}	UP	↓	↓	↓	↑	=	=
	DOWN	↓	↓	↑	↑	=	=
L_{in}	UP	=	=	=	↓	=	↑
	DOWN	=	=	=	=	=	↓
W_{sus}	UP	↓	=	↑	=	↑	↑
	DOWN	↓	=	↓	=	↑	↓
L_{sus}	UP	↓	=	↑	=	↑	↑
	DOWN	↓	=	↓	=	↑	↓

The same tests were carried out for an InsetFeed antenna as with the $\lambda/4$ antenna, and the results obtained are shown in Table 11.

Table 11. Result of the study of simulating the InsetFeed antenna with different input parameters.

Outputs		S11	BW	Directivity	Z	VSWR	Gain
Inputs							
W_p	UP	↓	↓	↑	=	Unclear	↑
	DOWN	↑	↑	↓	=	Unclear	↓
L_p	UP	↓	↑	↑	=	↑	↓
	DOWN	↑	↓	↓	=	↑	↑
L_{LT}	UP	=	=	↑	=	↑	↓
	DOWN	=	=	↓	=	↑	↑
W_{LT}	UP	=	=	=	↓	↑	=
	DOWN	=	=	=	↑	↑	=
Y_o	UP	=	↓	=	=	↑	↑
	DOWN	=	↓	=	=	↑	↓
g	UP	↑	↓	↑	=	↑	↓
	DOWN	↓	↓	↓	=	↓	↑
Distance Array	UP	↑	=	↑	=	↑	↑
	DOWN	↓	↓	↓	=	↑	↓

Table 11. Cont.

Outputs		S11	BW	Directivity	Z	VSWR	Gain
W_{in}	UP	↓	↓	↓	↑	=	=
	DOWN	↓	↓	↑	↑	=	=
L_{in}	UP	=	=	=	↓	=	↑
	DOWN	=	=	=	=	=	↓
W_{sus}	UP	↓	=	↑	=	↑	↑
	DOWN	↓	=	↓	=	↑	↓
L_{sus}	UP	↓	=	↑	=	↑	↑
	DOWN	↓	=	↓	=	↑	↓

Finally, the antennas' parameters are calculated and the antennas are simulated, obtaining the results that can be checked in the next Table 12.

Table 12. Inputs and outputs of the calculated and simulated parameters of the antenna arrays.

	2.4 GHz $\lambda/4$	2.4 GHz Inset	5.2 GHz $\lambda/4$	5.2 GHz Inset
Inputs				
W_p (mm)	32	32	25.2	22
L_p (mm)	35.54	35.68	16	16.16
W_{ia} (mm)	0.16	–	0.2	–
L_{ia} (mm)	18.04	–	8.28	–
W_{LT} (mm)	0.28	0.32	1.18	0.32
L_{LT} (mm)	0	18.04	5	8.3
Inset (mm)	–	11.5	–	6
g (mm)	–	0.6	–	0.16
W_{in}	1.3	1.2	1.3	1.2
L_{in}	3	3	3	2
LAMBDA	125	125	57.7	57.7
Distance Array	87.5	87.5	40.4	40.4
W_{sus}	137.5	137.5	75	75
L_{sus}	55	55	30	30
Outputs				
S11 (dB)	–32.4	–40	–38.66	–48
BW (MHz)	36	32	105	100
Z (Ω)	50.2	49.8	49.75	49.86
VSWR	1.05	1.02	1.02	1.01
Directivity (dB)	10.1	9.72	10.2	10.3
Gain (dBi)	4.65	4.78	8.16	8.22

As can be seen, the antenna arrays with a frequency of 5.2 GHz have better output characteristics than the 2.4 GHz antennas, especially in terms of gain or directivity. For this reason, the 5.2 GHz frequency with Inset Feed will be used to design a 2×1 array because it has a slightly better output characteristics, and its smaller size is also very important for the weight of the UAV.

5. Conclusions

Due to scientific and industrial interest, in the last years, many works have been developed to improve marine communications. However, these developments are unaffordable or difficult to put into practice.

In this paper, a study is made to verify the usefulness of a directive antenna and to explore ways to improve its design. Additionally, the process of coupling the antenna to a UAV to give it a higher altitude is studied, showing that it avoids experiencing shadowing and multipath fading.

It is verified in the simulation of the designed antennas that the calculated parameters are not as appropriate as required, and how, with the tests carried out, better results are achieved in their functional capabilities.

Two tables were specified to improve the output's characteristics of a patch antenna: Tables 6 and 7 for a patch antenna, and Tables 10 and 11 for a 2×1 array patch antenna. These tables determine how the increasing or decreasing of an input parameter affects an output parameter of the antenna. Thus, a maximum gain of 8.22 dBi and directivity of 10.3 dBi, with a frequency of 5.2 GHz was achieved in an array patch antenna InsetFeed with a flexible substrate such as PETG.

In future papers, the implementation of this antenna in the UAV will be studied in a smart antenna with a switched sweep through phase shifters to achieve greater directivity, knowing at all times the destination of reception and emission.

Author Contributions: L.G. was responsible for studying, analyse, design and simulate the patch antennas array. In addition, L.G. proposed and tested the EVD distribution to use it as the proving that the UAV better the marine communications, avoiding obstacles like fading or shadowing. A.S.I. has also participated in the validation of analysis of proposals, methods and discussion of results and reviewed the entire article and contributed to its translation. All authors have read and agreed to the published version of the manuscript.

Funding: This research received no external funding.

Acknowledgments: The development and completion of this work has been possible thanks to the vision and passion of Luis Antonio Mariscal, a telecommunications engineering professional from the University of Cadiz. In addition, the collaboration and help of Ahmed S. Ibrahim from Florida International University is also gratefully acknowledged.

Conflicts of Interest: The authors declare no conflict of interest.

References

1. Reyes-Guerrero, J.C.; Bruno, M.; Mariscal, L.A.; Medouri, A. Buoy-to-Ship Experimental Measurements over Sea at 5.8 GHz near Urban Environments. In Proceedings of the Mediterranean Microwave Symposium, Yasmine Hammamet, Tunisia, 8–10 September 2011; pp. 320–324.
2. Zhou, M.; Joe, J. Characterization of Radio Path Loss in Seaport Environment for WiMAX Applications. In Proceedings of the International Symposium on Antennas and Propagation, IEICE, Singapore, 1–4 November 2006; p. 176.
3. Reyes-Guerrero, J.C.; Mariscal, L.A. 5.8 GHz Propagation of Low-height Wireless Links in Sea Port Scenario. *Electron. Lett.* **2014**, *50*, 710–712. [\[CrossRef\]](#)
4. Reyes-Guerrero, J.C.; Sisul, G.; Mariscal, L.A. Measuring and Estimating the Propagation Path Loss and Shadowing Effects for Marine Wireless Sensor Networks at 5.8 GHz. In Proceedings of the 2012 20th Telecommunications Forum, TELFOR 2012, Belgrade, Serbia, 20–22 November 2012; pp. 323–326.
5. Erceg, V.; Hari, K.V.S.; Smith, M.S.; Baum, D.S.; Sheikh, K.; Tappenden, C.; Costa, J.M.; Bushue, C.; Sarajedini, A.; Schwartz, R.; et al. *Channel Models for Fixed Wireless Applications*; IEEE 802.16 Broadband Wireless Access Working Group; IEEE: New York, NY, USA, 2003.
6. Kim, Y.B.; Kim, J.H.; Wang, Y.P.; Chang, K.H.; Park, J.W.; Lim, Y.K. Application Scenarios of Nautical Ad-Hoc Network for Maritime Communications. In Proceedings of the OCEANS 2009, Biloxi, MS, USA, 26–29 October 2009; pp. 1–4.
7. Wang, L.; Li, B. UAV-Enabled Reliable Mobile Relaying under the Time-Varying Rician Fading Channel. *Alex. Eng. J.* **2023**, *64*, 771–783. [\[CrossRef\]](#)
8. Xu, G.; Zhang, N.; Xu, M.; Xu, Z.; Zhang, Q.; Song, Z. Outage Probability and Average BER of UAV-Assisted 727 Dual-Hop FSO Communication with Amplify-and-Forward Relaying. In *IEEE Transactions on Vehicular 728 Technology*; IEEE: New York, NY, USA, 2023. [\[CrossRef\]](#)
9. Qu, L.; Xu, G.; Zeng, Z.; Zhang, N.; Zhang, Q. UAV-Assisted RF/FSO Relay System for Space-Air-Ground 730 Integrated Network: A Performance Analysis. In *IEEE Transactions on Wireless Communications*; IEEE: New York, NY, USA, 2022; Volume 21, pp. 6211–6225. [\[CrossRef\]](#)
10. Ohmori, S.; Irimata, A.; Hase, Y.; Miura, M.; Kondo, K.; Morikawa, H. Characteristics of Sea Reflection Fading in Maritime Satellite Communications. *IEEE Trans. Antennas Propag.* **1985**, *33*, 838–845. [\[CrossRef\]](#)
11. Riheen, M.A.; Nguyen, T.T.; Saha, T.K.; Karacolak, T.; Sekhar, P.K. CPW Fed Wideband Bowtie Slot Antenna on PET Substrate. *Prog. Electromagn. Res. C* **2020**, *101*, 147–158. [\[CrossRef\]](#)

12. Ramly, A.M.; Malek, N.A.; Mohamad, S.Y.; Sukor, M.A. Design of a Circular Patch Antenna for 3D Printing. In Proceedings of the 2016 International Conference on Computer and Communication Engineering (ICCCCE), Kuala Lumpur, Malaysia, 26–27 July 2016; pp. 406–410.
13. Le, T.; Song, B.; Liu, Q.; Bahr, R.A.; Moscato, S.; Wong, C.P.; Tentzeris, M.M. A Novel Strain Sensor Based on 3D Printing Technology and 3D Antenna Design. In Proceedings of the Electronic Components and Technology Conference, San Diego, CA, USA, 26–29 May 2015; pp. 981–986.
14. Pizarro, F.; Salazar, R.; Rajo-Iglesias, E.; Rodriguez, M.; Fingerhuth, S.; Hermosilla, G. Parametric Study of 3D Additive Printing Parameters Using Conductive Filaments on Microwave Topologies. *IEEE Access* **2019**, *7*, 106814–106823. [[CrossRef](#)]
15. Kirtania, S.G.; Elger, A.W.; Hasan, M.R.; Wisniewska, A.; Sekhar, K.; Karacolak, T.; Sekhar, P.K. Flexible Antennas: A Review. *Micromachines* **2020**, *11*, 847. [[CrossRef](#)] [[PubMed](#)]
16. Dahle, R.; Ramadan, M. A Flexible 2.4 GHz Microstrip Patch Antenna Using a 3-D Printed Tile Array Design. In Proceedings of the IEEE MTT-S International Microwave Workshop Series on Advanced Materials and Processes (IMWS-AMP), Pavia, Italy, 20–22 September 2017; p. 3.
17. Bouchti, M. *El Diseño y Medición de Una Antena Wearable*; Universitat Politècnica de Catalunya: Terrasa, Spain, 2016.
18. Carrillo Morales, M. *Manual Carrillo Morales Agrupación de Antenas Microstrip para un Receptor SAR Biestatico*; Universidad Autónoma de Barcelona (UAB): Barcelona, Spain, 2010.
19. Obot, A.B.; Igwue, G.A.; Udofia, K.M. Design and Simulation of Rectangular Microstrip Antenna Arrays for Improved Gain Performance. *Int. J. Netw. Commun.* **2019**, *9*, 73–81. [[CrossRef](#)]
20. Elesawy, H.; Swelam, W.; Fouda, A.; Ismail, M. Hafez Design of Microstrip Array Antenna for Wireless Communication Application. *IOSR J. Eng.* **2013**, *3*, 1–7. [[CrossRef](#)]
21. Héctor Fabio Bermúdez, O.; Mario Alejandro Gómez, M.; Sebastián Botero, P. Tecnología de Microcintas Para Antenas, Caso de Diseño de un Dipolo en la Banda de 2.4 GHz. *ITECKNE* **2010**, *7*, 68–74. [[CrossRef](#)]
22. Nuñez, K.N.O. *Diseño, Modelado y Caracterización de Arreglo de Antenas Microstrip para Aplicaciones del Internet de las Cosas*; Instituto Nacional de Astrofísica, Óptica y Electrónica (INAOE): Puebla, México, 2019.
23. Vera Sánchez, J. *Diseño de una Agrupación Bidimensional de Antenas parche Rectangulares con Altadirectividad a 9.5 GHz*; Universidad Politécnica de Cartagena: Cartagena, Colombia, 2017.
24. Martín Luis, A.; Muschong Matías Andrés, A.; Sergio Luis, V.; Miguel, B. Diseño e Implementación de Antena Microstrip. In *Proceedings of the IX Congreso de Microelectrónica Aplicada, Buenos Aires, Argentina, 25–27 September 2019*; Lizárraga, E.M., Reinoso, C.S., Herrera, W.E., Eds.; Editorial Científica Universitaria de la Universidad Nacional de Catamarca: Catamarca, Argentina, 2019.
25. Barrera, B.E.R. *Diseño y Simulación de una Antena Microstrip de Rango de Operación de Super Altas Frecuencia (3.5 Ghz a 6 Ghz) para la Evaluación de la Tasa de Absorción Específica en Tejidos Humanos*; Universidad Católica de Colombia, Facultad de Ingeniería: Bogotá, Colombia, 2019.
26. Ramamurthy, V.; Katrodiya, D.V.; Peshavaria, J.N.; Ramamoorthy, V. Design of Microstrip Patch Antenna Array for Wireless Applications. *IJECT* **2015**, *6*, 61–64.
27. Parra Sonia Angelica, V.; Venegas López, B. *Diseño y Construcción de una Antena Tipo Patch en la Banda 712 de 5.4 Ghz*; Escuela Politécnica del Ejército: Sangolquí, Ecuador, 2011.
28. Nieto Escribano, J.M. *Diseño de un Array de Antenas parche con Alimentación en Serie a 60 GHz*; Universidad Pública de Navarra: Pamplona, Spain, 2018.
29. Rosado Sanz, J. *Diseño de un Array de Antenas de Parche de Banda Ancha en UHF para Sistemas Radar Pasivos*; Universidad de Alcalá, Escuela Politécnica Superior: Madrid, Spain, 2017.
30. Daniel, P.R.G. *Análisis Comparativo de Antenas Tipo Patch Con Tecnología Microstrip en la Banda X*; Universidad de las Fuerzas Armadas: Santo Domingo, Ecuador, 2018.
31. Viera, O.M. *Estudio y Aplicación del Cst Microwave Studio 5 Como 722 Herramienta de Simulación de Antenas*; Universidad Tecnológica de la Habana “José Antonio”: Habana, Cuba, 2007.
32. Balanis Constantine, A. *Antenna Theory Analysis and Design*, 3rd ed.; John Wiley & Sons, Inc.: Hoboken, NJ, USA, 2005; ISBN 0-471-66782-X.
33. James, J.R.; Hall, P.S. *Handbook of Microstrip Antennas*; Hall, J.R.J., Ed.; IEEE: London, UK, 1990.
34. James, J.R.; Hall, P.S.; Wood, C. *Microstrip Antenna Theory and Design*; Peter Peregrinus Ltd.: London, UK, 1982; ISBN 086341 088 X.
35. Galí, I.G. *Líneas de Transmisión*, Universidad Oberta de Cataluña, Barcelona. 2013. Available online: https://openaccess.uoc.edu/bitstream/10609/69445/6/Circuitos%20de%20microondas_M%C3%B3dulo%201_L%C3%ADneas%20de%20transmisi%C3%B3n.pdf (accessed on 13 February 2023).
36. Pieter, L.D.A. *The Design of Impedance-Matching Networks for Radio-Frequency and Microwave Amplifiers*, 1st ed.; Artech House Publishers: Norwood, MA, USA, 1985; ISBN 0890061726.

37. Fabio Bermudez Orozco, H. Desarrollo de Circuitos de RF Con Tecnología de Microcintas en la Banda de 2.4 GHz. *Colomb. Sci. Technol. Año XV* **2009**, *42*, 51–56.
38. Almodovar, S.J.Y. *Diseño de Antenas Direccionales de 2.4 y 5.8 GHz por Medio de la Técnica de Microcinta 720*; Universidad Autónoma de Ciudad Juárez: Juárez, Mexico, 2009.

Disclaimer/Publisher’s Note: The statements, opinions and data contained in all publications are solely those of the individual author(s) and contributor(s) and not of MDPI and/or the editor(s). MDPI and/or the editor(s) disclaim responsibility for any injury to people or property resulting from any ideas, methods, instructions or products referred to in the content.